CONCRETE LIBRARY OF JSCE NO. 31, JUNE 1998

NONDESTRUCTIVE EVALUATION OF FLAWS IN STEEL-CONCRETE COMPOSITE STRUCTURES

(Reprint from Proceedings of JSCE, No.564/V-35, May 1997)

Shigeyoshi NAGATAKI

Toshiro KAMADA

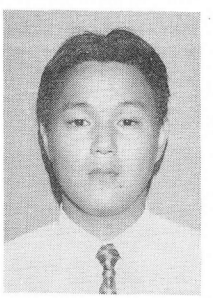

Gokichi YAZAKI

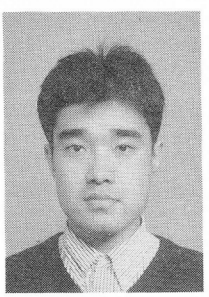

Motoi KUROSAKA

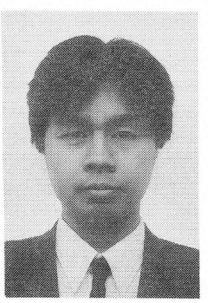

Mitsuyasu IWANAMI

In this paper, nondestructive evaluation methods for flaws in steel-concrete composite structures are investigated. The results demonstrate that cracks in the concrete in one section of concrete-filled steel rectangular tube beam can be detected by measuring the propagation time of the impact echo. Moreover, cracks wider than 0.2mm width can be confirmed by an X-ray technique. Further, it proves possible to check for delamination at the interface between the steel tube and concrete by measuring the thermal distribution on the steel surface with infrared thermography. Finally, it is confirmed that the acoustic emission (AE) technique is an effective way to evaluate flaws in steel-concrete composite structures in realtime.

Key words: nondestructive testing, steel-concrete composite structure, crack, delamination, impact echo, X-ray, infrared thermography, acoustic emission

JSCE and ACI Fellow S. Nagataki is professor emeritus of civil engineering at Tokyo Institute of Technology, and professor of civil engineering and architecture at Niigata University, Niigata, Japan. He received his doctor of engineering degree from the University of Tokyo in 1966. His research interests cover physical and chemical properties of concrete, durability of concrete, effective utilization of additives and nondestructive testing. Dr. Nagataki is a former chairman of the JSCE Committee on Concrete. He was awarded JSCE Yoshida prizes three times in 1972, 1987 and 1989, a JSCE thesis prize for a study on mechanism and prediction of deterioration of concrete in 1991.

T. Kamada is associate professor of civil engineering at Gifu University, Gifu, Japan. He received his doctor of engineering degree in 1997 from Tokyo Institute of Technology. His research work covers the nondestructive evaluation of concrete by ultrasonic testing, acoustic emission and thermography. He is a member of JSCE, JCI, JSNDI and JSMS.

G. Yazaki was a graduate student of civil engineering at Tokyo Institute of Technology, Tokyo, Japan. He received his master of engineering degree in 1996 from Tokyo Institute of Technology. He is a member of JSCE. He is now a civil engineer of Ministry of Construction, Japan.

M. Kurosaka was a graduate student of civil engineering at Tokyo Institute of Technology, Tokyo, Japan. He received his master of engineering degree in 1997 from Tokyo Institute of Technology. He is a member of JSCE. He is now a civil engineer of Tokyo Metropolitan Government, Japan.

M. Iwanami is a doctoral student of civil engineering at Tokyo Institute of Technology, Tokyo, Japan. He received his master of engineering degree in 1996 from Tokyo Institute of Technology. His research interests include nondestructive evaluation methods for concrete structures. He is a member of JSCE, JCI and JSNDI.

1. INTRODUCTION

Steel-concrete composite structures [1,2] have very high strength and ductility, and they offer exceptional seismic performance. Designed to take best advantage of the complementary characteristics of concrete and steel, they make it possible to reduce the cross-section of structural members as compared with ordinary RC structures. As such, these structures satisfy many contemporary demands such as improvements to structure appearance, better utilization of space around structures, and increased construction speed. Moreover, they are also being applied to the seismic retrofitting of bridge columns for improved ductility, which have been carried out extensively in Japan since the Hyogoken Nambu Earthquake of 1995 [3].

It is clear that steel-concrete composites have considerable potential for use in a variety of structures, and fairly extensive studies have recently been carried out on design methods, mechanical properties, and durability [4,5]. Most of these studies, however, focused on the mechanical behavior of particular members, which depend on the condition of the bond between steel and concrete and the type of linkage between members, etc. Despite this, few evaluation methods for flaws in steel-concrete composite structures have been investigated so far, although they are of great importance to exhibit their expected performance appropriately. In some structures, the concrete is fully enclosed with steel, so it is impossible to evaluate the deterioration in concrete and the condition of the steel-concrete bond by visual inspection. Hence, there is an immediate need for nondestructive evaluation techniques for flaws in these structures to be established.

In this study, nondestructive methods were investigated for their ability to evaluate flaws in steel-concrete composites, and especially in concrete-filled steel rectangular tubes where the concrete part is fully enclosed in the steel tube. Particular attention was paid to cracks in the internal concrete and to delamination between the steel tube and concrete. For these two types of defects, evaluation methods suitable for both regular inspections and realtime monitoring are proposed.

2. EVALUATION OF CRACKS IN ENCLOSED CONCRETE

Concrete-filled steel rectangular tube beams were used for this study. As shown in Fig.1, the concrete was enclosed in rectangular steel tube of 4.5mm thickness, and mixing was carried out under the following conditions: W/C=40% and s/a=41%. To induce cracks in the concrete inside the steel tube, a bending force was applied to the beams until 25, 50, 75, and 100% of the failure load was reached.

Ultrasonic testing is one very effective means of evaluating cracks in concrete [6]. However, in the case of concrete-filled steel tube beams, the interface between steel and concrete interferes with propagation of the ultrasonic pulses through the specimen. This makes it impossible to measure the propagating time, a precequisite for determining the location of cracks. For this reason, ultrasonic testing was thought to be unsuitable for the evaluation of cracks in this case. Hence, in this study, we investigate the applicability of the impact-echo technique and the X-ray technique to the evaluation of cracks. Moreover, in order to confirm the validity of the results, the actual crack pattern in concrete was observed after removing part of the steel tube.

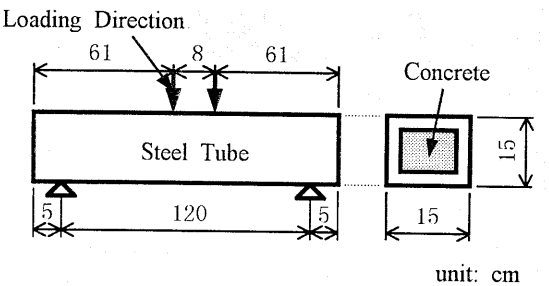

Fig.1 Outline of Specimen Used

2.1 Outline of Experiment

a) Impact-echo Technique

The impact-echo technique involves measuring the propagation time of an elastic wave transmitted through the concrete to determine the location of cracks. However, concrete-filled steel tubes have two transmission paths: through the steel and concrete. Since the propagating velocity in steel is larger than that in concrete, it is impossible to measure the arrival time of elastic waves propagating through the concrete. Therefore, in this study, the elastic waves were introduced as shown in Fig.2. After small holes 5mm in diameter were drilled in the steel tube, one end of a steel rod 2mm in diameter was placed on the concrete surface and other end was struck with a hammer. The elastic waves generated in this manner were detected by two AE sensors attached on the top and bottom surfaces of the beam. The location of cracks was estimated by the difference in arrival time of the elastic waves detected by two sensors. Measurements were conducted for six paths, as shown in Fig.3.

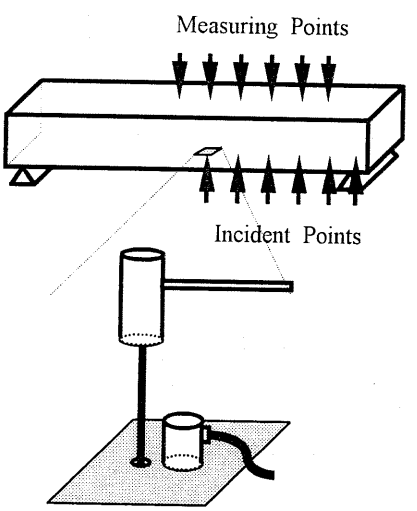

Fig.2 Incidence of Elastic Waves

b) X-ray Technique

In general, the existence of cracks in concrete can be evaluated from the contrast of X-ray photographs, due to differences in the amount of radiation transmitted. With this technique, it is important to optimize the X-ray dose according to what is being evaluated. In order to determine the most appropriate dose for concrete-filled steel tubes, the exposure times of 5, 10, and 20 minutes were tried with the X-ray tube voltage and distance between X-ray source and specimen kept constant; 300kV and 85cm, respectively. The X-ray photo-graphs were taken using an industrial X-ray system (PS300; manufactured by Philips Japan, Ltd.), with industrial X-ray film (sensitivity: #100, size: 25.4*30.5(cm)), and an X-ray grid of 2mm thickness. The side surface of the specimen was exposed to radiation to make it easy to evaluate the location of cracks and their size.

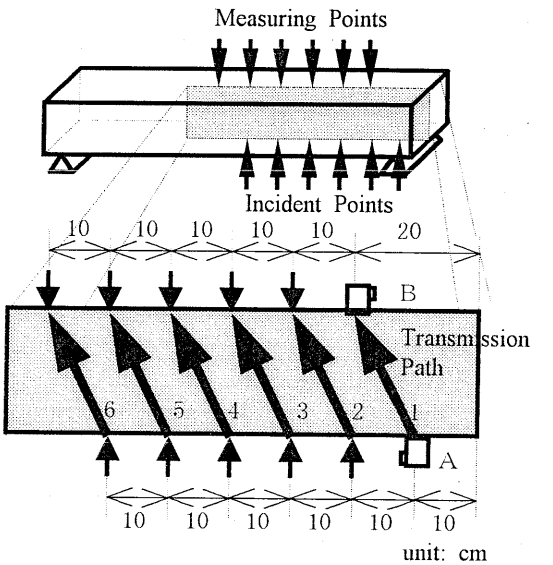

Fig.3 Measurement of Propagation Time of Elastic Waves through Concrete

c) Visual Observation

The actual crack patterns in concrete within the steel tubes loaded to the predetermined levels were observed after cutting away part of the surface of the steel tube using a diamond saw (see Fig.4).

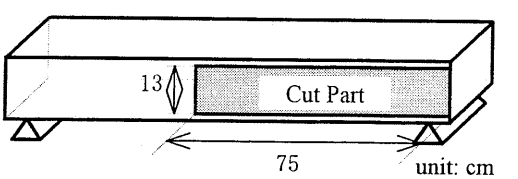

Fig.4 Cut Part for Visual Observation of Internal Concrete

2.2 Results and Discussion

a) Examination by Impact-echo Technique

Table 1 shows the difference in measured arrival time between the two AE sensors for the specimen loaded to failure. On paths near the end of the beam, which was considered comparatively sound, the amount of scatter in the measured values was within 5 μs. On the other hand, on paths near the center of the beam, that became larger. This is because the elastic wave did not propagate through the shortest path due to the existence of cracks. To take the scattering in the measured values into account, the average of the six measurements was employed as an evaluation index, removing the two largest and two smallest values from the total of ten measurements.

The average arrival time difference on each path is shown in Fig.5. For Paths 1-4, the arrival time difference was almost constant. On the other hand, the values for paths near the center of the beam were apparently larger than those for paths near the end. From this, it was concluded that cracks had occurred around the center of the beam, and that there existed no cracks near the end.

Table 1 Arrival Time Difference of Elastic Wave for Each Path

	Path 1	Path 2	Path 3	Path 4	Path 5	Path 6
	70	70	75	72	80	80
	74	68	70	75	80	80
	70	75	73	73	82	80
	73	75	73	68	85	85
	70	70	70	75	75	78
	72	75	65	65	80	88
Average	71.5	72.2	71.0	71.3	80.3	81.8

unit: μsec

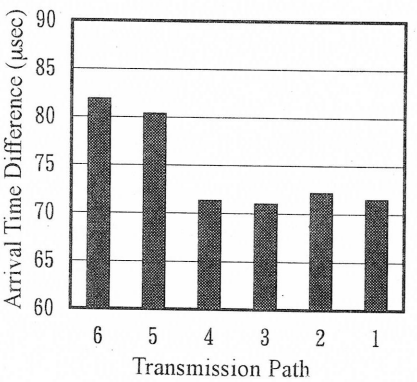

Fig.5 Average Arrival Time Difference for Each Path

The application of this method to locate cracks in an actual structure would require advance measurement of propagation time where the concrete is sound. Further, efforts are needed to develop a method that allows the steel surface itself to be impacted without drilling a hole in the tube. Frequency analysis of the received signals should make it possible to distinguish the waves passing through the concrete.

b) Examination of X-ray Technique

Within the limits of this study, exposure times of 5 and 20 minutes gave no clear image of the cracks on the X-ray photographs. With a 10-minute exposure, however, crack images were seen on the films for the specimen loaded up to the failure load, as shown in Photo.1. In case of specimens loaded up

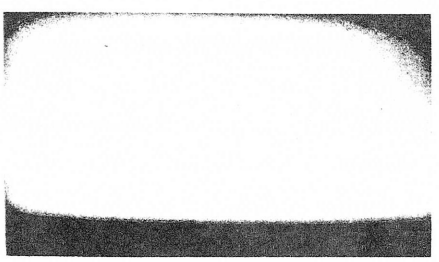

Load Level: 25%

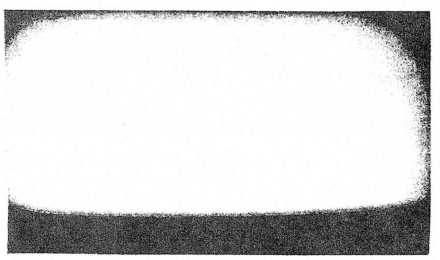

Load Level: 75%

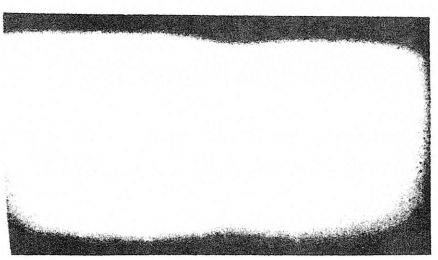

Load Level: 50%

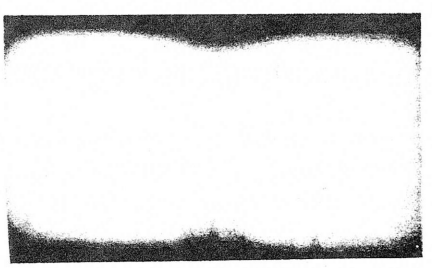

Load Level: 100%

Photo 1 X-ray Photographs

to the levels of 25,50, and 75% of the failure load, it was impossible to confirm the existence of cracks in concrete on the films.

c) Confirmation through Visual Observation

Photo.2 shows the result of visual observations for the specimen loaded up to each level. These photos verify that cracks in the internal concrete progressed and increased in number as the load level rose. The impact-echo technique indicated that the specimen loaded up to failure suffered cracks around the center of the beam, while no cracking occurred near the end. This correlates well the results of this visual observations, demonstrating that the location of cracks can be estimated by the impact-echo technique.

A comparison with the results of the X-ray technique also supports the applicability of this technique. Cracks more than 0.2mm in width were confirmed, while it was impossible to detect cracks less than 0.2mm. Where cracks existed only near the surface, however, it was difficult to detect them regardless of their width. The use of a contrast medium is proposed as a way to evaluate cracks in detail.

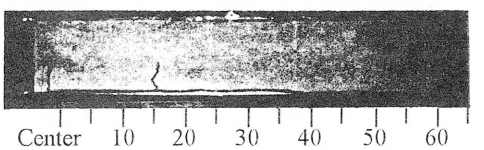

Load Level: 25%

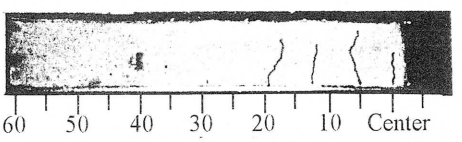

Load Level: 50%

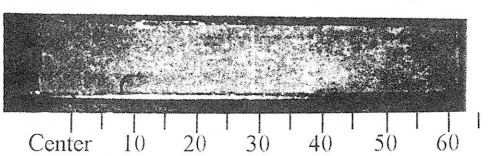

Load Level: 75%

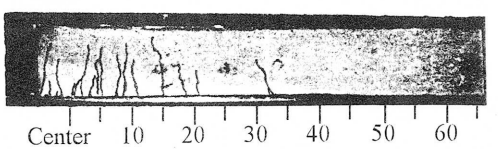

Load Level: 100%

unit: cm

Photo 2 Visual Observations

3. EVALUATION OF DELAMINATION BETWEEN STEEL AND CONCRETE

In this chapter, a method of evaluating delamination between steel and concrete by the infrared thermographic technique is investigated. The thermal distribution over the surface of the steel tube beams was measured to estimate the state of delamination.

3.1 Outline of Experiment

Beam specimens as shown in Fig.1 were also used for this experiment. Infrared thermographic measurement were carried out on specimens loaded up to the predetermined load levels: 25, 50, 75,

and 100% of the ultimate bending load. The progress of delamination as the load increased was evaluated from the thermal distribution on the steel surface. A thermal video system (TVS2300Mk II ST; manufactured by Nippon Avionics Co., LTD.) was used for these measurements. To ensure that delamination showed up in the thermal distribution, the surface temperature of the specimen was artificially raised by applying a heat load immediately prior to thermographic measurements. Taking into consideration the finding of a previous study on the application of thermography to concrete structures [7] and also the characteristic of steel-concrete composite structures, this application of heat load had to meet the following conditions:

(1) The heat load must instantaneously change the temperature in the steel surface only.

(2) The heat load must be constant over the whole surface.

(3) The heat load should be as high as possible.

To meet these conditions, it was concluded that the best method would be to use liquid nitrogen as a coolant for the steel surface of the specimens. In the experiment, liquid nitrogen was absorbed into a towel wound around a plywood board (9*25*130 (cm)). This board was then pressed against the steel surface for 10 seconds at constant pressure prior to measurements.

After the measurements, the actual amount of delamination between steel and concrete was determined. An epoxy-resin filler was poured into the delamination of the specimen loaded up to the failure load. As shown in Fig.6, small holes 4mm in diameter were drilled on the top surface of the beam for this purpose. After the filler had hardened, part of the steel tube was cut away and the hardened filler picked out. The thickness of the hardened filler was measured using calipers and a microscope.

3.2 Results and Discussion

The thermal distribution at the surface of specimens loaded up to each level is shown in Fig.7. In the case of specimens loaded up to 25, 50, and 75% of the failure load, the temperature near the center of the beam was lower than that

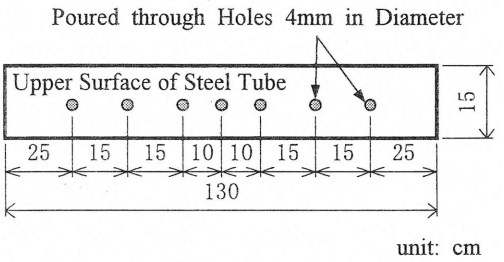

Fig.6 Pouring Epoxy-Resin Filler into Delamination Part


Load Level: 0%

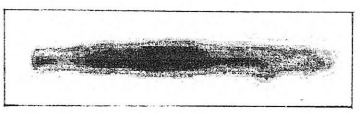
Load Level: 25%

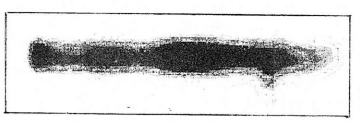
Load Level: 50%


Load Level: 75%

Load Level: 100%

(unit: °C)

Fig.7 Thermal Distribution on Upper Surface of Steel Tube

around the ends. This indicates that delamination began near the center of the beam. However, there is no difference in temperatures in these three cases. The explanation for this is that the degree of delamination for each specimen was almost the same after unloading due to elastic deformation of the steel tube. On the other hand, in the case of the specimen loaded up to the failure load, a marked drop in temperature can be seen at the center of the beam. This is where buckling of the steel tube took place, as shown in Fig.8. It is thought that the greater delamination caused by this buckling disturbed the transmission of heat, resulting in a considerable decrease in temperature at these points. Compared with the results for the other load levels, the drop in temperature for the specimen loaded to failure was much greater overall. This is because the amount of delamination was greater over the whole beam due to plastic deformation of the steel tube after yielding.

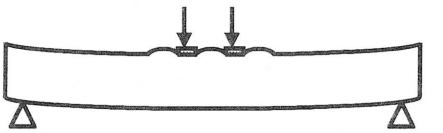

Fig.8 Yielding of Steel Tube

The degree of delamination estimated from these thermal distributions was confirmed based on actual thickness measurements made by pouring an epoxy-resin filler into the space. Photo.3 shows the state of the hardened filler inside the steel tube. Thus, at the center of the beam where the temperature was exceedingly low, the thickness of the filler was about 3mm. At the edge of the beam, it was about 0.1mm.
This demonstrates the possibility of estimating the amount of delamination by infrared thermography. It appears that delaminations of more than about 0.1mm can be detected within the limits of this study.

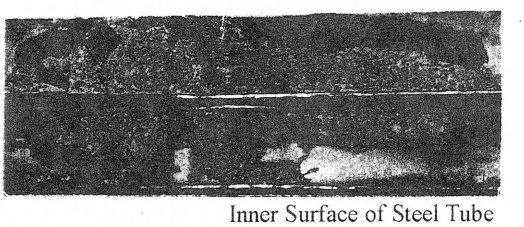

Photo 3 State of Hardened Filler inside Steel Tube

Other factors are likely to affect the results of such measurements; ambient conditions, the cooling method, the thickness of the steel, and so on. It will be necessary to examine an appropriate arrangement of measuring conditions in detail.

4. APPLICATION OF AE TECHNIQUE TO MONITORING FLAWS IN STEEL-CONCRETE COMPOSITE STRUCTURES

In this chapter, a method of assessing the occurrence and development of flaws using an AE technique is investigated with the aim of monitoring flaws in steel-concrete composite structures. The AE technique is thought to be ideal for monitoring flaws such as cracks and delaminations, since measurements can be automatically taken over a wide range once a simple sensor setup has been completed. In this study, a method is studied for classifying the AE signals that occur during bending into three types: delamination between steel and concrete, slip between steel and concrete, and concrete cracking. The AE characteristics of delamination and slip are also investigated through model tests.

4.1 Outline of Experiment

a) Delamination Model Test

The specimen used for this test is shown in Fig.9. It was made by laying mortar on a steel pate of 4.5mm thickness. The mix proportion of mortar was W/C=40% and S/C=2.0. Before jointing mortar to the plate, the area was roughened by sawing in order to ensure a good joint between the steel plate and mortar. Tensile force was applied to the two ends of the steel plate to cause delamination between the steel plate and mortar, during which AE signals were measured by AE sensors mounted on the steel plate as shown in the figure. Noise from the anchored ends of the steel plate was eliminated based on the results of AE source location analysis.

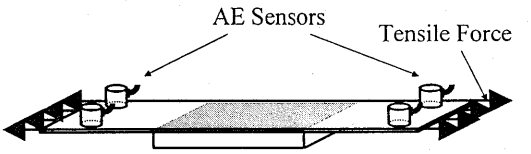

Fig.9 Model Test for Delamination between Steel and Concrete

b) Slip Model Test

Fig.10 shows the specimen used for this test. This steel-concrete composite specimen was made by simply applying compression load to the steel-concrete interface using a vise. Accordingly, there was no actual bond between the steel plate and concrete, but mechanical friction. As indicated in the figure, a shear force was applied to the steel plate and concrete to induce slippage between them. A Teflon sheet 0.1mm in thickness was inserted in appropriate locations to prevent noise.

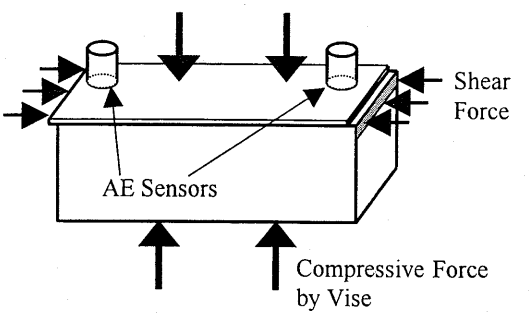

Fig.10 Model Test for Slip between Steel and Concrete

c) Bending Test on Concrete-Filled Steel Tube Beam

As in Fig.1, a bending force was applied to the beams until the top surface of the steel tube reached the buckling point and started to deform plastically. AE measurements were carried out during loading. Similar measurements were performed on other specimens loaded up to 25% and 50% of the failure load. AE sensors were located as shown in Fig.11, with Sensors 1 and 6 attached to the surface of the concrete, and Sensors 2-5 attached to the surface of the steel tube.

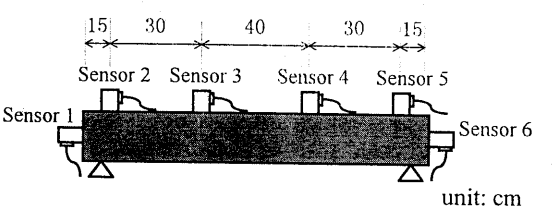

Fig.11 Location of AE Sensors

d) AE Measurement

The AE measuring system used was a LOCAN320, manufactured by Nippon Physical Acoustics Ltd. The AE signals detected by the sensors (R15; manufactured by Nippon Physical Acoustics Ltd.) with a resonant frequency of 150kHz were passed through a 100kHz high-pass filter and a 40dB-gain pre-amplifer. In the main-amplifer, the signals were boosted by 30dB, so the total gain was 70dB. The threshold was set at a level of 50dB.

4.2 Results and Discussion

a) Evaluation of AE Characteristics due to Delamination and Slip

Fig.12 shows the frequency distribution and the cumulative curve of the risetime of AE signals measured during the delamination model test. A risetime was defined as the time from the first crossing of the threshold to the peak of the AE signal. In this figure, the risetime corresponding to the 80% point on the cumulative curve is about 50μs. Fig.13 gives results for a similar analysis on the slip model test. Here, the risetime corresponding to the 80% point on the cumulative curve is 125μs. Thus, the risetime of AE signals generated by delamination and slip is quite short, and AE signals with particularly short risetimes are predominantly generated when delamination occurs. Accordingly, the risetime of AE signal can be considered effective as a way to discriminate the signals due to delamination and slip.

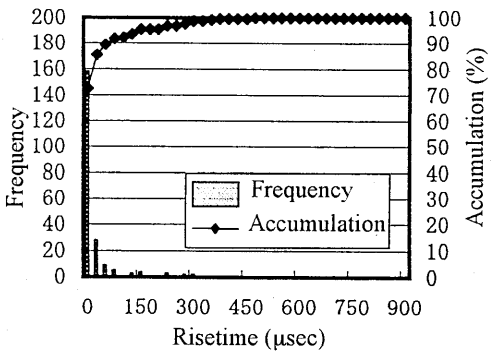

Fig.12 Frequency Distribution of Risetime (Delamination Model Test)

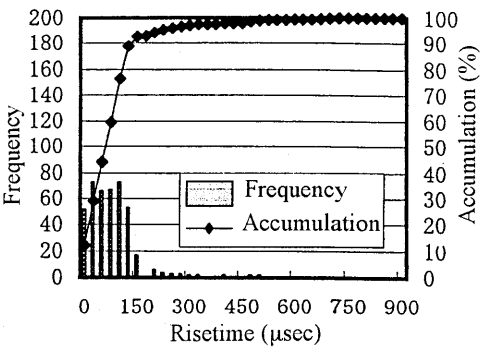

Fig.13 Frequency Distribution of Risetime (Slip Model Test)

b) Evaluation of Location and Scale of Cracks

Fig.14 shows the change in AE hits during the bending test as time elapsed. This clarifies that AE activity peaked at elapsed times of 50,65, and 335 seconds. These AE signals are thought to have been caused by the occurrence of bending cracks. The applied load corresponding to these elapsed times was 33,40 and 195kN, respectively. This demonstrates that the cracking in concrete can be evaluated by AE activity.

In this study, AE energy which was defined as the area of the enveloped AE waveform was investigated to evaluate the scale of cracking. According to a previous study [8], it is known that the scale of cracking can be estimated by this waveform parameter. Also, one-dimensional AE source location analysis was carried out on the AE results from the bending test using the arrival time interval between Sensors 2 and 5. The AE energy was also calculated for signals received by the nearest sensor to the source as estimated from the result of one-dimensional location analysis. Fig.15 and 16 show the relationships between calculated AE source and AE energy as a function of elapsed time for the beams loaded until 25% and

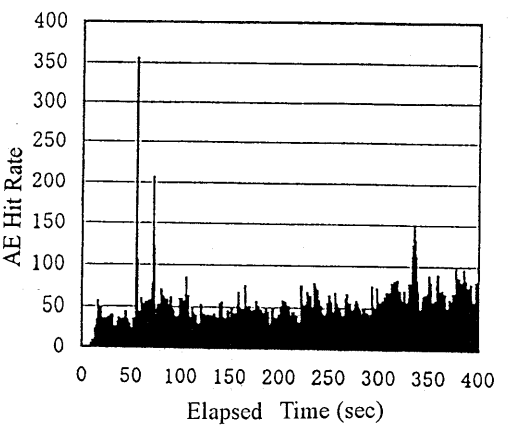

Fig.14 AE Behavior during Bending Test

50% of the failure load. Furthermore, the visual observations of cracks in the concrete are shown as well as an aid to comprehension of the graphs above. In these figures, the X position is defined as the distance from Sensor 2 at the end of the beam, and X=50, and 100 correspond to the center of the beam and other end (Sensor 5), respectively. Thus, in the case of the beam loaded until 25%, it was found that cracks were present near X=50 and 65 through actual observations. This corresponds well with the result of AE source location analysis, suggesting the occurrence of large-scale cracks. This demonstrates that the occurrence of cracks in the internal concrete can be well estimated by AE source location analysis. After cracking began, AE signals with relatively large energy occurred continuously near X=50 for 40 seconds and also near X=65 for an elapsed time of 120-165 seconds. These AE signals are thought to have been caused by crack development. Thus, it is clarified that AE energy is appropriate way to evaluate the fracture process of concrete-filled steel tube beams. Similarly, in the case of the beam loaded up to 50%, the existence of cracks was observed visually near X=40, and the occurrence of AE was recognized at the same point by AE source location analysis.

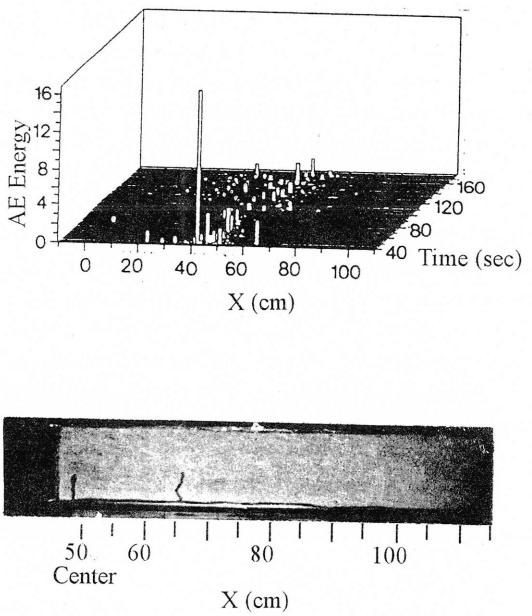

Fig. 15 Relationship between AE Source and AE Energy as a Function of Elapsed Time (Load Level: 25%)

This application of AE source location and AE energy as evaluation indices indicates good potential for the evaluation of the location and scale of concrete cracking in steel-concrete composite structures.

c) Discrimination of AE Causes during Bending Test

The model tests indicated that it is possible to distinguish two causes of AE signals: delamination and slip. In the case of steel-concrete composite structures, the AE signals caused by concrete cracking also need to be isolated. Thus, AE signals thought to have been caused by cracking in the previous section were analyzed using the risetime as a means of discrimination, as mentioned before. In this case, it was a time of 400 μs that corresponded to the 80% point on the cumulative curve. This is considerably longer than for delamination or slip, because of the attenuation of AE signals propagating through the concrete. On this

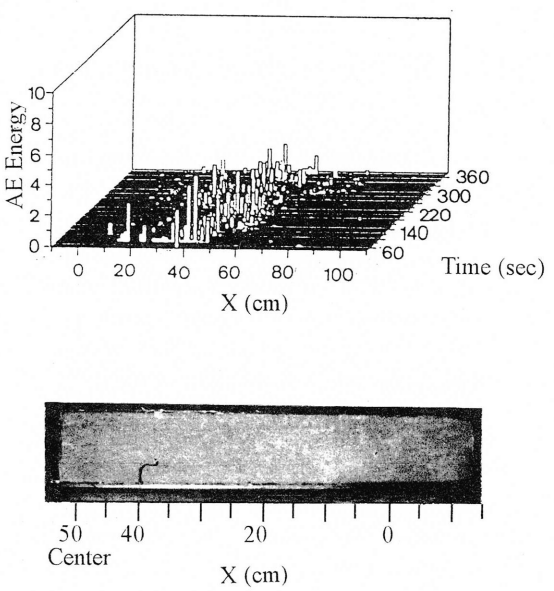

Fig. 16 Relationship between AE Source and AE Energy as a Function of Elapsed Time (Load Level: 50%)

basis, the risetime of AE signals was used to discriminate the dominant cause of AE signals detected during a particular time interval regarded as a group.

Several typical phenomena occurring during the fracture process of concrete-filled steel tube beams were evaluated by this method of risetime measurement. First, at the beginning of a bending test on a beam loaded up to ultimate failure, the frequency distribution and the cumulative curve were calculated. The result is shown in Fig.18. The risetime corresponding to the 80% point on the cumulative curve was 325 μs, which is closer to the value for cracking than that for delamination or slip. This led to the conclusion that, at this early stage of the bending test, the occurrence of cracks in the concrete was dominant. The steel-concrete interfaces near the cracking then delaminated or slipped later. This corresponds well with the thermography results in the previous chapter. Next, Fig.19 shows the frequency distribution and cumulative curve of risetime for AE signals detected during unloading, when cracking and delamination would not be expected to occur. In this figure, the risetime corresponding to the 80% point is 100μs, which is extremely close to the value for the slip model test. Therefore, it is concluded that slip between the steel tube and concrete occurred.

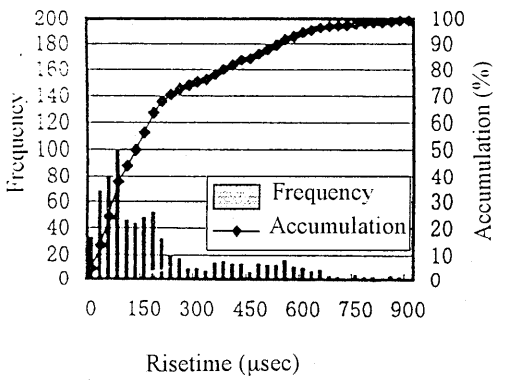

Fig.17 Frequency Distribution of Risetime (Cracking in Concrete)

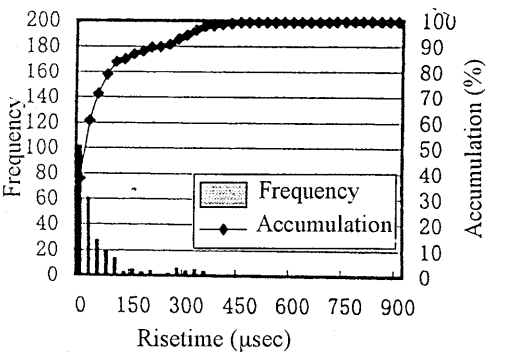

Fig.18 Frequency Distribution of Risetime (Bending Test)

These results verify that the frequency distribution and the cumulative curve of the risetime are useful for discriminating the dominant causes of AE signals. However, as mentioned before, this method is not proposed as a way to determine the cause of individual AE signals, but for estimating the dominant cause of AE signals regarded as a group. Thus, when this method is used to evaluate flaws in existing structures, it is necessary to deal with the AE data as a group by a pattern recognition technique on the basis of probability theory.

In this study, the interval of AE sensors was identical for all cases of model test specimens and concrete-filled steel tube beams, so the effect of attenuation of AE signals as they propagated through the concrete was not taken into consideration. However, when applying this method to existing structures, the correction for this attenuation should be made by reference to the results of AE source location analysis.

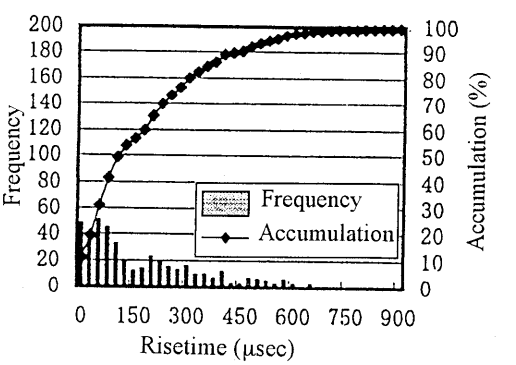

Fig.19 Frequency Distribution of Risetime (Unloading)

5. CONCLUSIONS

In evaluating the flaws in steel-concrete composite structures, it is a matter of great importance to select the appropriate method for each type of flaw. Within the limits of this study, the following conclusions related to the nondestructive evaluation of certain kinds of flaw in steel-concrete composite structures were obtained.

(1) The impact-echo technique proved capable of roughly estimating the location of cracks in concrete, even though the concrete was fully enclosed in steel.
(2) Cracks in the concrete exceeding 0.2mm in width, could be detected by the X-ray technique.
(3) The amount of delamination at the steel-concrete interface was evaluated by the thermal distribution on the steel surface as measured by infrared thermography.
(4) AE measurement provide useful information concerning the location and scale of cracks in concrete, and also their process of development.
(5) It was possible to distinguish the dominant causes of the AE signals: delamination or slip at the steel-concrete interface or cracking in the concrete: by using the AE waveform parameter "risetime" as an evaluation index.

REFERENCES

[1] JSCE: Guidelines for Design of Steel-Concrete Composite Structures, 1989 (in Japanese)
[2] ACI: Building Code Requirements of Reinforced Concrete, ACI 318-89, pp.130-131
[3] N. Matsumoto and T. Sato: Current Status of Seismic Strengthing Methods for Railway Reinforced Concrete Viaducts, Concrete Journal, Vol.35, No.10, pp.9-17, 1997 (in Japanese)
[4] H. Yokota and O. Kiyomiya: Strength and Crack Behaviors of Steel-Concrete Hybrid Beams, Proceedings of JSCE, No.451/V-17, pp.149-158, 1992 (in Japanese)
[5] M. Shams and M. A. Saadeghvaziri: State of the Art of Concrete-Filled Steel Tubular Columns, ACI Structural Journal, Vol.94, No.5, pp.558-571, 1997
[6] British Standards Institution: Recommendations for Non-destructive Methods of Test for Concrete - The Measurement of the Velocity of Ultrasonic Pulses in Concrete, BS 4408, Part 5, 1974
[7] M. Yanai and T. Uomoto: Fundamental Studies on the Use of Heat-Infrared Ray Technique to Determine the Condition of Voids and Reinforcement in Concrete Structures, Proceedings of JSCE, No. 442/V-16, pp.91-100, 1992 (in Japanese)
[8] T. Kamada, S. Nagataki, and N. Otsuki: Evaluation of Delamination at Interface Between Old Concrete and Repair Material by Non-destructive Testing Methods, Proceedings of Second CANMET/ACI International Symposium on Advances in Concrete Technology, pp.469-479, 1995